



## RESEARCH ARTICLE

### Histopathological Investigation of Feline Oral Squamous Cell Carcinoma and the Possible Role of Papillomavirus Infection

H Ozturk-Gurgen<sup>1</sup>, O Almilli<sup>2</sup>, G Sennazli<sup>1</sup> and M Majzoub-Altweck<sup>2†</sup>

<sup>1</sup>Istanbul University-Cerrahpasa, Department of Veterinary Pathology, Faculty of Veterinary Medicine, TR-34500 Istanbul, Turkey; <sup>2</sup>Ludwig Maximilian University of Munich, Institute of Veterinary Pathology, Faculty of Veterinary Medicine, DE-80539 Munich, Germany

\*Corresponding author: hazal.ozturkgurgen@iuc.edu.tr

#### ARTICLE HISTORY (21-182)

Received: April 26, 2021  
Revised: August 31, 2021  
Accepted: October 11, 2021  
Published online: November 14, 2021

#### Key words:

Cat  
Grading  
Histology  
Oral  
Papillomavirus  
Tumor

#### ABSTRACT

The histopathological subtyping and grading of oral squamous cell carcinoma are well established in human medicine, but there are currently no standard classification and grading schema used for oral squamous cell carcinoma in cats. In this study, it was aimed to investigate different subtypes and grades of feline oral squamous cell carcinoma and the possible role of the papillomavirus infection in the progression of this tumor by using the methods of histopathology, immunohistochemistry, and transmission electron microscopy. Out of the 32 tissue samples, conventional (14/31; 43.75%), verrucous (8/32; 25%), papillary (5/32; 15.62%), acantholytic (3/32; 9.37%), and adenosquamous (2/32; 6.25%) subtypes of the tumor were determined in the affected cats. Grading of the tumor was performed according to Anneroth's and Bryne's systems and revealed that there was no relationship between histopathological subtypes and grades of the cases. Histopathologic findings suggestive of papillomavirus infection were determined not only in verrucous and papillary subtypes as seen in human medicine, but also in different other subtypes of the tumor. Moreover, immunopositivity for papillomavirus was obtained from the conventional, acantholytic, and adenosquamous subtypes of the tumor. In conclusion, the relationship between grading and subtypes of oral squamous cell carcinoma observed in this study showed differences in comparison with the human counterparts. The effect of papillomavirus infection in the progression of oral squamous cell carcinoma remained uncertain.

**To Cite This Article:** Ozturk-Gurgen H, Almilli O, Sennazli G and Majzoub-Altweck M, 2022. Histopathological investigation of feline oral squamous cell carcinoma and the possible role of papillomavirus infection. Pak Vet J, 42(1): 95-101. <http://dx.doi.org/10.29261/pakvetj/2021.077>

#### INTRODUCTION

Oral squamous cell carcinoma (OSCC) is the most common oropharyngeal malignancy encountered in humans, presenting 90% of the oral tumors (Ferlay *et al.*, 2018). Likewise, feline OSCC represents the most common oral neoplasm seen in older cats (Wingo, 2018; Mikiewicz *et al.*, 2019). Most affected sites have been determined to be sublingual areas, mandibular and maxillary areas (Bilgic *et al.*, 2015).

Feline OSCC has been found similar to the human head and neck tumor since both cancers show aggressive clinical behavior with local invasion, metastasis, and recurrence (Wypij, 2013). Histopathologic evaluation of OSCC is performed based on different histopathologic subtypes and grading systems, which indicate

characteristic histopathological properties for each subtype (Pereira *et al.*, 2007; Doshi *et al.*, 2011) in human medicine. The first grading system developed by Broders depends on the malignant differentiation of the tumor cells and includes four groups presenting the degree of differentiation from well-differentiated to anaplastic levels (Doshi *et al.*, 2011). However, it has been assumed that this grading system has no correlation with the clinical history of the patients (Doshi *et al.*, 2011). With this regard, the multifactorial grading system according to the structure, differentiation, nuclear pleomorphism, mitosis, mode of invasion, stage of invasion, vascular invasion, and lymphoplasmacytic infiltration of the tumor has been developed by Jacobsson (Doshi *et al.*, 2011) and then has been updated as Anneroth's multifactorial grading system (Doshi *et al.*, 2011). Eventually, Bryne *et al.* (1992) has

used this multifactorial grading system not for the whole area of the tumor, but only for the deep areas of invasions (Doshi *et al.*, 2011). The idea of Bryne's system suggests that neoplastic cells of deeply invasive parts of a tumor may have more tumor characteristics than those of metastases (Bryne *et al.*, 1992).

In human medicine, verrucous type of OSCC, which is a well-differentiated variant of the tumor (Saito *et al.*, 1999), has been found related to papillomavirus (PV) infection that has been considered as one of the causative factors for developing squamous cell carcinoma on mucosal tissues of head and neck region (Gillison, 2000). In veterinary medicine, the possible relationship between PV and OSCC has previously been reported in cats (Munday *et al.*, 2009; O'Neill *et al.*, 2011). Histological features of the papillary subtype have been mostly found in association with the possible PV infection, but there is currently no evidence to support this hypothesis (Munday *et al.*, 2017).

In this study, it was aimed to investigate the histopathological features of feline SCC in the head and neck region through the classification scheme of subtyping and grading systems, and to compare the relationship between these subtypes with the possible role of papillomavirus infection. The study was performed based on histopathological properties of OSCC, histological changes suggestive of PV infection, the immune reactivity of neoplastic cells against PV antigen using immunohistochemistry, and viral particles sought by transmission electron microscopy (TEM).

## MATERIALS AND METHODS

### Tissue samples and evaluation of patient profiles:

Anamnesis and information of biopsy materials taken from the head and neck region of 32 cats diagnosed with SCC were compiled from the archives of the Institute of Veterinary Pathology at the Centre of Veterinary Medicine of the Ludwig Maximilian University of Munich. The patients were evaluated according to their breed, gender, age, and the localization of the tumor. Genders of the cats were categorized as male, castrated male, female, and spayed female.

**Histopathologic examination:** Histopathological examination was performed according to the histological features of OSCC and suggestive alterations induced by PV infection. The histological subtyping was performed according to the classification of subtypes for human

(Barnes *et al.*, 2005; Pereira *et al.*, 2007) and canine OSCC (Nemec *et al.*, 2012): i) conventional type, ii) verrucous type iii) papillary type iv) basoloid type v) spindle type vi) other variants. The neoplastic samples were graded by both Anneroth's 1987 and Bryne's 1992 classification criteria (Table 1), and the cases were divided into 3 groups as Grade I, Grade II, and Grade III (Table 2). The scoring of the mitotic index was determined by counting mitotic cells in 10/400 high magnification field (HPF) followed by the mean value (Table 1) for an HPF, which is one of the grading criteria of the Anneroth system.

The relationship between the possible role of PV infection and the occurrence of OSCC was evaluated according to the subtypes of OSCC encountered in this study and histological changes suggestive of PV infection, such as the thickening of the epithelium, the existence of koilocytes, eosinophilic intranuclear inclusion bodies, and immunopositivity obtained by immunohistochemistry.

**Immunohistochemical analysis:** The immunohistochemistry for papillomavirus antigen (Papillomavirus HPV+BPV antibody, PA5-35416, Thermo Fisher Scientific) was performed for all tissue samples using a standard protocol for the Avidin-Biotin-Complex method. Sections of 4 µm thickness were dewaxed in xylol and rehydrated in a descending alcohol series (100%, 90%, 70% alcohol). Antigen retrieval procedure was performed using citrate buffer (10mM, pH 6.0, with Tween 20) at 800 W in a microwave oven (2 X 10 min). Subsequently, slides were treated with 1% hydrogen peroxide (15 min) to block endogenous peroxidase activity and then washed with 0.5 M, pH 7.6 tris buffered saline (TBS). Sections were pre-incubated with normal rabbit serum (MP Biomedicals, Germany) at room temperature (30 min), followed by incubation at room temperature with a 1:100 dilution of polyclonal antibody human and bovine papillomavirus (HPV+BPV) (60 min). Sections were then washed with TBS, incubated with a 1:100 dilution of seconder polyclonal antibody rabbit anti-goat IgPO (Dako, Germany) (50 min). Sections were then washed again with TBS. The binding of the secondary antibody was visualized by the reaction with hydrogen peroxide and 3,3' diaminobenzidine tetrahydrochloride dihydrate (DAB) (Kem-En-Tec Diagnostics, Germany) as a chromogen. Slides were counterstained with Mayer's hematoxylin. A case with papillomavirus containing canine oral papillomavirus served as a positive control, and no primary antibody was applied to the sections that were running as negative controls for each turn.

**Table 1:** Evaluation criteria of multifactorial grading systems by Anneroth *et al.* (1987) and Bryne *et al.* (1992)

Anneroth <i>et al.</i> (1987) for whole thickness of the tumor	Bryne <i>et al.</i> (1992) for deep invasive cells
Tumor cell population	Tumor cell population
Keratinization (scored from 1-4)*	Keratinization (scored from 1-4)
Nuclear pleomorphism (scored from 1-4)**	Nuclear pleomorphism (scored from 1-4)
Number of mitosis (scored from 1-4)***	-
Tumor - host relationship	Tumor - host relationship
Pattern of invasion (scored from 1-4)°	Pattern of invasion (scored from 1-4)
Stage of invasion (scored from 1-4)°°	-
Lymphocytic infiltration (scored from 1-4)°°°	Lymphocytic infiltration (scored from 1-4)°°°

\*Scoring of keratinization; 1: >50% cells keratinized, 2: 20-50 % cells keratinized, 3: 5-20% cells keratinized and as 4: 0-5 % cells keratinized.\*\*Scoring of nuclear pleomorphism; 1: few pleomorphism, 2: Moderately abundant pleomorphism, 3: Abundant pleomorphism and 4: Extreme pleomorphism.\*\*\* Scoring of number of mitosis; 1: 0-1 mitosis/hpf, 2: 2-3 mitosis/hpf, 3: 4-5 mitosis /hpf and 4: >5 mitosis/hpf. ° Scoring of pattern of invasion; 1: Well- delineated infiltrating borders, 2: Infiltrating, solid cords, bands and/or strands, 3: Small groups or cords of infiltrating cells and 4: Marked and diffuse cellular invasion. °° Scoring of stage of invasion; 1: Carcinoma-in-situ, 2: Distinct invasion, but involving lamina propria only, 3: Invasion below lamina propria and 4: Extensive and deep invasion replacing most of the stromal tissue and infiltrating jawbone. °°° Scoring of lymphocytic infiltration; 1: Marked, 2: Moderate, 3: Slight and 4: None.

**Transmission Electron Microscopy (TEM):**

Transmission electron microscopy was performed on 2 out of 5 cases with a striking positive immune reaction to locate viral particles. For this purpose, positive areas were microscopically determined in tissue samples, and approximately 1 mm<sup>3</sup> of paraffin-embedded tissue sample was removed from these areas using special pliers, and then embedded in epoxy resin. One micrometer of tissue sections was prepared and stained by toluidine blue-safranin staining for light microscopy to select sites for electron microscopic evaluation. Ultra-thin sections were stained with uranyl-acetate and lead citrate. In the last stage, corresponding immunolabeled areas and cells were sought for the existence of the particles of papillomavirus.

**Statistical analyses:** A chi-square test was performed to evaluate associations between the subtypes and the categorical variables of patients' profiles, tumor localization, and immunohistochemical positivity of the papillomavirus. In order to implement the chi-square test, tumor subtypes were regrouped as conventional and non-

conventional, and age scales were divided into 7-10 years and >10 years. When the chi-square test was not appropriate despite the combination of the groups, a fisher's exact test was performed, and this method was used to evaluate associations between the subtypes and histopathological changes suggestive of papillomavirus infection, such as the existence of koilocytes and inclusion bodies, and also between the subtypes and the grading systems.

**RESULTS**

**Patient profiles:** The predominantly affected breed was the European shorthair cat (22/32). The age of the patients varied from 7 to 17 years old and the average age was 10.2. The most common gender was determined as male castrated (16/32), followed by the spayed female (7/32). The most (13/32) affected localization was the tongue (Table 3). There were no significant differences between the subtypes and the profile of the patients, and the tumor localization ( $P>0.005$ ).

**Table 2:** Sum of scores for multifactorial grading systems by Anneroth *et al.* (1987) and Bryne *et al.* (1992)

Sum of score for Anneroth <i>et al.</i> (1987)	6-12: Grade I 13-18: Grade II 19-24: Grade III	Sum of score for Bryne <i>et al.</i> (1992)	4-8: Grade I 9-12: Grade II 13-16: Grade III
--	--	---	--

**Table 3:** Patient profiles, histopathologic grading, and PV associated changes observed in the affected cats with OSCC. (C: Case; Loc: Localization; MGS: Multifactorial grading system; Ko: Koilocytes; Incl. b.: Inclusion bodies; CM: Castrated male; M: Male; SF: Spayed female; F: Female; NA: Not available, ESH: European shorthair)

Case	Loc	Age	Gender	Breed	Anneroth's MGS	Bryne's MGS	Ko	Incl. b.	IHC-PV
<b>Conventional</b>									
C. 1	Tongue	16	CM	NA	3	3	-	+	-
C. 2	Gingiva	10	CM	ESH	2	2	-	+	-
C. 3	Tongue	14	CM	NA	2	1	-	-	-
C. 4	Tongue	13.5	F	ESH	3	3	-	+	-
C. 5	Tongue	14	CM	ESH	3	3	-	+	-
C. 6	Lip-mucosa	10	CM	ESH	2	2	-	+	-
C. 7	Tongue	13.5	CM	ESH	2	2	-	-	+
C. 8	Tongue	7.5	CM	ESH	2	2	-	-	+
C. 9	Oral cavity	7	CM	ESH	2	2	-	-	-
C. 10	Tongue	9	SF	Persian	2	2	-	+	-
C. 11	Gingiva	15.5	CM	Norwegian forest cat	1	1	-	-	-
C. 12	Oral cavity	17	SF	ESH	2	2	-	-	+
C. 13	Gingiva	10	M	ESH	3	3	-	+	-
C. 14	Mandibula	14	SF	ESH	1	1	-	-	-
<b>Verrucous</b>									
C. 15	Maxilla	17	NA	NA	2	2	+	+	-
C. 16	Tongue	7	CM	ESH	2	2	+	+	-
C. 17	Oral cavity	17	F	ESH	2	2	-	+	-
C. 18	Oral cavity	NA	CM	ESH	2	2	+	+	-
C. 19	Tongue	15	SF	ESH	2	2	-	+	-
C. 20	Mandibula	14	SF	ESH	2	2	-	+	-
C. 21	Tongue	14	CM	Norwegian forest cat	2	2	-	-	-
C. 22	Tongue-mandibula	13	SF	ESH	2	2	+	+	-
<b>Papillary</b>									
C. 23	Tongue	13	CM	NA	1	1	+	-	-
C. 24	Gingiva	13	CM	ESH	2	2	-	-	-
C. 25	Nasal sinus	NA	NA	NA	1	2	-	+	-
C. 26	Oral cavity	NA	NA	NA	2	2	-	+	-
C. 27	Larynx	8	CM	ESH	2	2	-	+	-
<b>Achantolytic</b>									
C. 28	Oral cavity	12	CM	ESH	2	2	-	+	+
C. 29	Gingiva	15	M	Maine coon	2	2	-	+	+
C. 30	Oral cavity	15	F	ESH	1	1	-	-	-
<b>Adenosquamous</b>									
C. 31	Tongue	14	SF	ESH	1	1	-	+	-
C. 32	Nose	7	M	ESH	2	2	-	-	-

**Histopathological findings:** Histopathological examination revealed different subtypes of OSCC, which were conventional, verrucous, papillary, acantholytic, and adenosquamous (Table 3). Conventional subtype was found to be the most common subtype in this study, which was also statistically supported ( $P=0.001$ ). When subtypes and histopathological grading systems were compared, conventional subtype showed significant differences with grade III malignancy by both grading systems ( $P>0.05$ ).

Fourteen out of 32 (43.75%) cases appeared as trabeculae and nests of epithelial cells extending into the submucosa, and so they were diagnosed as the conventional type of OSCC (Fig. 1). Nuclear pleomorphism showed variation from mild to extreme (3/14: mild; 2/14: moderate; 4/14: abundant; 5/14: extreme). The number of mitosis in an HPF was found as 0-1 in 7/14, 2-5 in 3/14, and more than 5 in 4/14 of the cases. Keratinization of the tumors was scored as 1 in 1/14, 2 in 3/14, 3 in 4/14, and 4 in 6/14 of the cases. The pattern of invasion was commonly seen as small groups, bands, or cords of infiltrating cells. Only a few cases showed well-delineated infiltrating borders, and also marked and widespread cellular dissemination. The invasion of adjacent tissue was seen in only 4/14 cases, 1/14 cases showed invasion into the lymphatic vessels, and 2/14 cases indicated deep invasion infiltrating the jawbone. Lymphocytic infiltration was marked in 8/14 of the cases, moderate in 2/14 of the cases, one case showed mild lymphocytic infiltration, and the rest (3/14 of the cases) had none. According to these histopathological findings, 2/14 of the cases were classified as Grade I, 7/14 of the cases were found as Grade II, and 4/14 of the cases were classified as Grade III according to Anneroth's and Bryne's multifactorial grading system. Only one of the cases was found as Grade II for Anneroth's and as Grade I for Bryne's system (Table 3).

Eight out of 32 cases (25%) were found compatible with verrucous OSCC, which was diagnosed based on the existence of an exophytic growth and development from the basal layer with broad tongues of mature squamous epithelium by pushing into underlying tissue (Fig. 2). Abundant nuclear pleomorphism of the neoplastic cells was distinct in 4/8 cases, the rest showed little (2/8), moderate (1/8), and extreme (1/8) nuclear pleomorphism. The number of mitosis in an HPF was commonly scored as 2 or 3. Keratinization of the neoplastic cells was scored as 2 in 3/8, as 3 in 1/8, and as 4 in 4/8 of the cases. The pattern of invasion was commonly seen as small groups, bands or cords of infiltrating cells, or marked and widespread cellular dissemination into the deep mucosa and adjacent tissues. The invasion of adjacent tissue was seen in lamina propria only for 5/8 cases. In addition, 1/8 cases showed invasion into the lymphatic vessel, and 2/8 cases showed deep invasion infiltrating the jawbone. Lymphocytic infiltration was generally found as marked and moderate. Only 1/8 cases showed mild infiltration. According to these histopathological findings, all verrucous subtypes were found to be associated with Grade II for both Anneroth's and Bryne's multifactorial grading system (Table 3).

Papillary type of OSCC was characterized by papillary growth pattern and was observed in 5/32 cases

(15.62%). The parameter was the presence of a predominant papillary growth pattern for the diagnosis of this type (Fig. 3). Nuclear pleomorphism was observed from moderate (1/5) to abundant (4/5) and commonly with moderate mitotic numbers (scored as 2). Keratinization was usually minimal. Distinct keratinization was observed only in 1/5 cases. The pattern of invasion was seen as small groups, bands or cords of infiltrating cells. Marked and widespread cellular dissemination was seen only in 1/5 cases. Grading of this subtype indicated Grade I (2/5) and Grade II (3/5) according to Anneroth's system, and Grade I (1/5) and Grade II (4/5) according to Bryne's system.

Acantholytic type of OSCC (Fig. 4) was found in 3/32 cases (9.37%). This type was diagnosed depending on the acantholytic cells located in cystic spaces lined by neoplastic squamous cells. Nuclear pleomorphism was abundant in 2/3 cases and mild in the other case. Mitotic count was found different in each case, between 1 to 3, and keratinization was distinctive in 1/3 cases and moderate in other 2/3 cases. The pattern of invasion was commonly seen as small groups and bands. One of the cases had an invasion in adjacent muscle tissue and jawbone. All of the cases were found as Grade II according to both Anneroth's and Bryne's multifactorial grading systems.

Two out of 32 cases (6.25%) were found as the adenosquamous type of SCC (Fig. 5), which was characterized by the tubular epithelial structures with anastomosing islands and sheets of keratinizing neoplastic epithelium. Nuclear pleomorphism was mild in one and extreme in the other case. Mitotic count was found mild, but no keratinization was observed in both cases. The pattern of invasion was commonly seen as small groups and bands groups, or cords of infiltrating cells.

Histopathological changes suggestive of papillomavirus infection were characterized by thickening of the epithelium, as seen in the verrucous subtype of OSCC, eosinophilic intracytoplasmic inclusion bodies (Fig. 1, insert), and koilocytes. Inclusion bodies were seen in 20/32 cases in all subtypes. Koilocytes were observed in verrucous, 4/8 cases, and papillary subtypes, 1/5 cases, of OSCC. There were no significant differences identified by the histopathological changes, the existence of koilocytes and inclusion bodies, and the subtypes. ( $P$ -value for existence of koilocytes  $>0.05$ ;  $P$ -value for existence of inclusion bodies  $>0.05$ ).

**Immunohistochemical Findings:** Immunohistochemistry against PV obtained positive intracellular dark brown immunoreaction (Fig. 6) in 5/32 cases, among 3 of which were conventional and 2 were acantholytic subtypes of OSCC. There were no cases in which inclusion bodies, koilocytes, and immunopositivity were the common findings. There was no significant difference identified by the IHC results and subgroups ( $P>0.05$ ).

**Findings of Transmission Electron Microscopy:** There was no evidence of the papillomaviral particles in either of the 2 cases with good immunopositivity in TEM examinations.

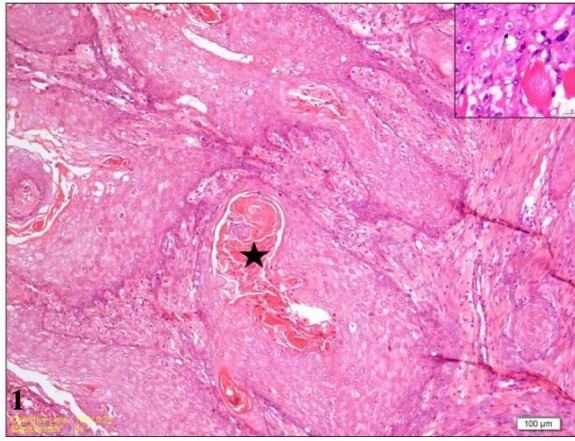


**Fig. 1:** Conventional subtype of OSCC showing nests of malignant epithelial cells with moderate keratinization (star; score for keratinization: 2), Grade II (for both Anneroth and Bryne’s multifactorial grading system), tongue. Bar = 100µm. Insert; an intranuclearly located eosinophilic inclusion body (arrow). Bar = 10 µm.

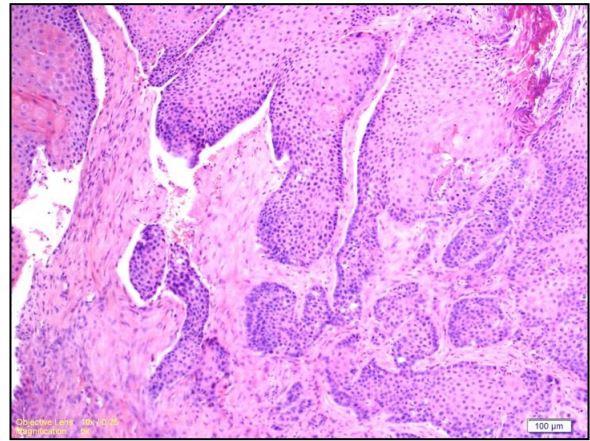


**Fig. 2:** Verrucous subtype of OSCC indicating the development from the basal layer with broad tongues of mature squamous epithelium by pushing into underlying tissue with score 3 for the pattern of invasion, tongue. Bar = 100 µm.

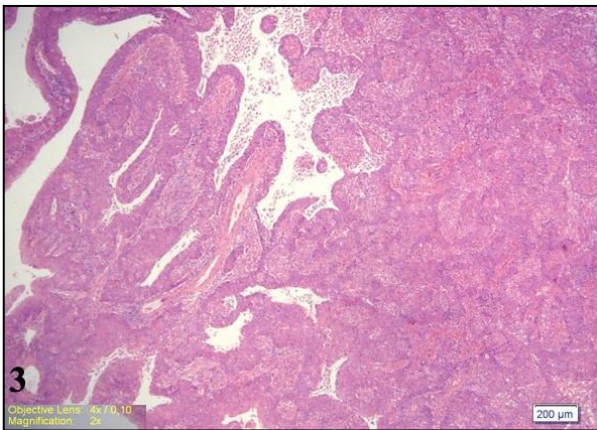


**Fig. 3:** Papillary subtype of OSCC, predominant papillary growth pattern, larynx. Bar = 200 µm.

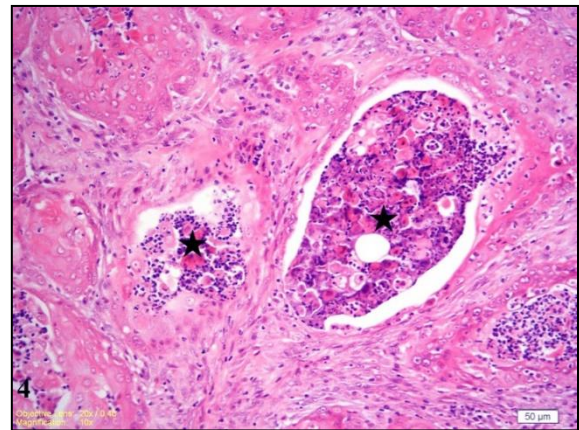


**Fig. 4:** Acantholytic subtype of OSCC, cystic spaces contain acantholytic cells (stars) surrounded by neoplastic squamous cells, oral cavity. Bar = 50 µm.

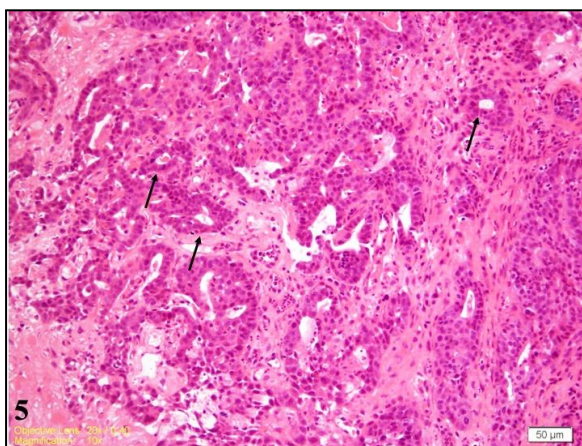


**Fig. 5:** Adenosquamous subtype of OSCC, neoplastic squamous cells built glandular structures (arrows), tongue. Bar = 50 µm.

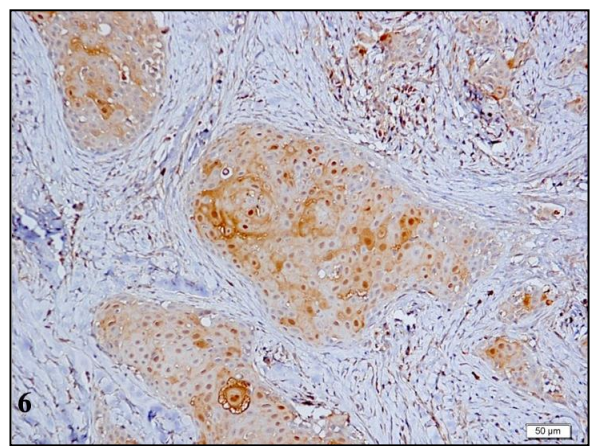


**Fig. 6:** Intranuclear positive reaction for papillomavirus infection. Bar = 50 µm.

**DISCUSSION**

This retrospective study presents the commonly affected localization, histopathologic subtyping, and grading of the feline OSCC, and compares the possible role of papillomavirus infection with the encountered subtypes of the tumor. Previously, feline OSCC has been

determined as the most common oral malignant tumor occurring in older cats, without any sex and breed predilection (Wingo, 2018; Mikiewicz *et al.*, 2019). The most commonly affected localizations have been described as maxillary, mandibular, and lingual or sublingual regions (Hayes *et al.*, 2007). In this study, the average age of the patients was found compatible with the

previous studies (O'Neill *et al.*, 2011, Munday *et al.*, 2011; Wingo, 2018; Mikiewicz *et al.*, 2019). In this study, the most commonly encountered breed and sex were European short hair and castrated male, respectively. The most affected localization for OSCC was determined as tongue, as previously indicated (Bilgic *et al.*, 2015). However, no significant differences between the subgroups and patients' profiles and tumor localization were identified by statistical analyses.

In veterinary medicine, evaluation of OSCC, regarding subtyping or grading of the tumor, has similarities with human medicine (Munday *et al.*, 2017). In this study, 5 subtypes with different histopathologic characteristics could be defined, and the conventional subtype was found significantly more than other groups, which was found compatible with previous studies reported in cats, and dogs (Nemec *et al.* 2012; Munday *et al.*, 2019).

The histopathological grading system of OSCC in veterinary medicine is performed regarding cellular and nuclear pleomorphism, degree of keratinization, and mitotic rate only if the tumor is classified under the conventional subtype of OSCC (Munday *et al.*, 2017). However, it has not been developed for routine diagnostics. In this study, the relationship between histopathological malignancy and these different subtypes of feline OSCC was documented by grading the tumor accordingly to both Anneroth's and Bryne's multifactorial grading systems in human medicine (Doshi *et al.*, 2011). It was observed that conventional type OSCC showed from well- to poorly-differentiated malignancy criteria, as described in human medicine. In comparison with the non-conventional subtypes, the conventional variant showed much higher grade (Grade III) or poorly differentiated according to both grading systems, which is also supported statistically. On the other hand, the surprising finding was that verrucous and papillary subtypes, known as well-differentiated variants in human medicine (Pereira *et al.*, 2007), were associated with the intermediate grade (Grade II) or moderately-differentiated for all verrucous, and most of the papillary subtypes in this study. Furthermore, unlike in the human counterpart, they invaded aggressively in local deep tissue and showed an osteolytic growth pattern.

The effect of PV infection on the development of OSCC has been investigated in most studies (Munday *et al.*, 2009, 2011; O'Neill *et al.*, 2011; Munday and French, 2015; Yamashita-Kawanishi *et al.*, 2018; Munday *et al.*, 2019; Chu *et al.*, 2020), but the possible role of PV in the development of OSCC has been associated with only a small number of patients (Chu *et al.*, 2020). The PV induced lesions can be determined by cytopathologic effects of the virus and intranuclear eosinophilic inclusion bodies (Munday and French, 2015). In addition to the histopathological properties, demonstration of PV infection by immunohistochemistry (Munday and French, 2015) and detection of papillomaviral DNA have been performed with the OSCC in cats (O'Neill *et al.*, 2011; Chu *et al.*, 2020). In human medicine, the verrucous subtype is related to the PV infection, especially in association with tobacco and alcohol consumption (Eisenberg *et al.*, 1985), which possesses an important

role for the development in the head and neck region (Gillison *et al.*, 2000; Devaraja *et al.*, 2003). The relationship between the papillomavirus and different subtypes of the feline OSCC was investigated by IHC and TEM in this study. However, there was no correlation between the histopathologic subtypes and histopathologic findings suggestive of PV-induced cases, and no significant correlation was determined by statistical analyses either. Immunopositive cases were found in conventional and acantholytic subtypes, rather than in verrucous or papillary subtypes. In addition, no correlation with PV-induced cytopathologic changes and immunohistochemistry was observed, and no viral particle was found by TEM in the immunopositive cases. The reason for the negative immune results could be related to the latent PV infection or infection with minimal replication. In a study, PV has been sought in cats with Bowenoid in-situ carcinoma, and the negative IHC results in some of these lesions have been interpreted as 'hit and run' model of the virus, which is presumed to be an initial cellular transformation by the virus and a subsequent loss of viral genome (Wilhelm *et al.*, 2006). The present study lacks the confirmation of histopathologic findings suggestive of PV-induced neoplastic lesions, and IHC positive cases by the amplification of papillomaviral DNA, as indicated previously in other studies feline OSCC (Munday *et al.*, 2009; O'Neill *et al.*, 2011). Nevertheless, the actual role of papillomavirus remains questionable for veterinary medicine (Munday *et al.*, 2009, 2011; O'Neill *et al.*, 2011; Munday and French, 2015; Altamura *et al.*, 2016, Chu *et al.*, 2020).

**Conclusions:** This study presents the histopathological interpretation of the feline OSCC regarding subtyping and grading of the tumor. Unlike in human medicine, verrucous and papillary subtypes of OSCC in this study could indicate malign features and were found mostly referred to as Grade II. Histopathological changes suggestive of PV infection were observed in most of the verrucous and papillary subtypes of the tumor, but the immunopositive reaction was observed in the conventional subtype of the tumor. However, due to the small number of cases in this study, further studies should be carried out by achieving statistically significant differences. In addition, the question that should be asked for further studies is whether the PV has a role in the progression of OSCC. If so, whether the subtype should be related to the verrucous or papillary subtypes of OSCC, or whether it is also possible to have the same effect in conventional, and other types of OSCC.

**Acknowledgments:** The authors would like to thank Dr. İsmail Dal for his contribution to the development of statistical analyses.

**Authors contribution:** HOG designed the study, HOG, and OAM compiled the cases from the databases of the Pathology Department of the Veterinary Faculty. HOG, OAM, GS, and MMA analyzed and graphed the cases, and all the authors critically revised the manuscript for important contents and approved the final version.

## REFERENCES

- Anneroth G and Hansen LS, 1984. A methodologic study of histologic classification and grading of malignancy in oral squamous cell carcinoma. *Eur J Oral Sci* 92:448-68.
- Altamura G, Eleni C, Meoli R, *et al.*, 2018. Tongue squamous cell carcinoma in a European lynx (*Lynx lynx*): Papillomavirus infection and histologic analysis. *Vet Sci* 5:1.
- Barnes L, Eveson JW, Reichart P, *et al.*, 2005. Pathology and genetics of head and neck tumors. In: World Health Organization Classification of Tumors. IARC Press, Lyon, France, pp:107-208.
- Bilgic O, Duda L, Sánchez MD, *et al.*, 2015. Feline oral squamous cell carcinoma: clinical manifestations and literature review. *J Vet Dent* 32:30-40.
- Bryne M, Koppang HS, Lilleng R, *et al.*, 1992. Malignancy grading of the deep invasive margins of oral squamous cell carcinomas has high prognostic value. *J Pathol* 166:375-81.
- Chu S, Wylie TN, Wylie KM, *et al.*, 2020. A virome sequencing approach to feline oral squamous cell carcinoma to evaluate viral causative factors. *Vet Microbiol* Available from <https://doi.org/10.1016/j.vetmic.2019.108491>.
- Devaraja K, Aggarwal S, Verma SS, *et al.*, 2020. Clinico-pathological peculiarities of human papilloma virus driven head and neck squamous cell carcinoma: A comprehensive update. *Life Sci* 245:117383.
- Doshi NP, Shah SA, Patel KB *et al.*, 2011. Histological grading of oral cancer: A comparison of different systems and their relation to lymph node metastasis. *Indian J Community Med* 2:136-42.
- Eisenberg E, Barry R and David JK, 1985. Verrucous carcinoma: A possible viral pathogenesis. *Oral Surg Oral Med Oral Pathol Oral Radiol* 59:52-7.
- Ferlay J, Colombet M, Soerjomataram I, *et al.*, 2019. Estimating the global cancer incidence and mortality in 2018: Globocan sources and methods. *Int J Cancer* 144:1941-53.
- Gillison ML, Koch WM, Capone RB, *et al.*, 2000. Evidence for a causal association between human papillomavirus and a subset of head and neck cancers. *J Natl Cancer Inst* 92:709-20.
- Hayes AM, Adams VJ, Scase TJ, *et al.*, 2007. Survival of 54 cats with oral squamous cell carcinoma in United Kingdom general practice. *J Small Anim Pract* 48:394-9.
- Mikiewicz M, Paździor Czapula K, Gesek M, *et al.*, 2019. Canine and feline oral cavity tumors and tumor-like lesions: a retrospective study of 486 cases (2015-2017). *J Comp Pathol* 172:80-7.
- Munday JS, Dunowska M and De Grey S, 2009. Detection of two different papillomaviruses within a feline cutaneous squamous cell carcinoma: Case report and review of the literature. *N Z Vet J* 57:248-51.
- Munday JS, French AF, Peters-Kennedy J, *et al.*, 2011. Increased p16CDKN2A protein within feline cutaneous viral plaques, bowenoid in situ carcinomas, and a subset of invasive squamous cell carcinomas. *Vet Pathol* 48:460-5.
- Munday JS and French AF, 2015. *Felis catus* papillomavirus types 1 and 4 are rarely present in neoplastic and inflammatory oral lesions of cats. *Res Vet Sci* 100:220-2.
- Munday JS, Löhr CV and Kiupel M, 2017. Tumors of the alimentary tract. In: *Tumors in Domestic Animals: (Meuten DJ, ed) 5th Ed*, John Wiley and Sons, Inc. Ames, Iowa, USA, pp:500-9.
- Munday JS, He Y, Aberdein D, *et al.*, 2019. Increased p16CDKN2A, but not p53, immunostaining is predictive of longer survival time in cats with oral squamous cell carcinomas. *Vet J* 248:64-70.
- Nemec A, Murphy B, Kass PH, *et al.*, 2012. Histological subtypes of oral non-tonsillar squamous cell carcinoma in dogs. *J Comp Pathol* 147:111-20.
- O'Neill SH, Newkirk KM, Anis EA, *et al.*, 2011. Detection of human papillomavirus DNA in feline premalignant and invasive squamous cell carcinoma. *Vet Dermatol* 22:68-74.
- Pereira CM, Oliveira DT, Landman G, *et al.*, 2007. Histologic subtypes of oral squamous cell carcinoma: prognostic relevance. *J Can Dent Assoc* 73:339-44.
- Saito T, Nakajima T and Mogi K 1999. Immunohistochemical analysis of cell cycle-associated proteins p16, pRb, p53, p27 and Ki-67 in oral cancer and precancer with special reference to verrucous carcinomas. *J Oral Pathol Med* 28:226-32.
- Wilhelm S, Degorce-Rubiales F, Godson D, *et al.*, 2006. Clinical, histological and immunohistochemical study of feline viral plaques and bowenoid in situ carcinomas. *Vet Dermatol* 17:424-31.
- Wingo K, 2018. Histopathologic diagnoses from biopsies of the oral cavity in 403 dogs and 73 cats. *J Vent Dent* 35:7-17.
- Wypij JM 2013. A naturally occurring feline model of head and neck squamous cell carcinoma. *Patholog Res Int* Available from: <http://dx.doi.org/10.1155/2013/502197>.
- Yamashita-Kawanishi N, Sawanobori R, Matsumiya K, *et al.*, 2018. Detection of *Felis catus* papillomavirus type 3 and 4 DNA from squamous cell carcinoma cases of cats in Japan. *J Vet Med Sci* Available from: <https://doi.org/10.1292/jvms.18-0089>.